Static and Dynamical Valence-Charge-Density Properties of GaAs*

Ullrich Pietsch

Universität Potsdam, FB Physik, Am Neuen Palais 10, D-O-1571 Potsdam, Germany

Z. Naturforsch. **48a**, 29–37 (1993); received December 5, 1991

Owing to the close neighbourhood of Ga and As in Mendeleev's table, GaAs shows two fundamental classes of X-ray structure amplitudes distinguished by their extremely different scattering power. They are differently sensitive to the valence electron density (VED) redistribution caused by the chemical bond and must be measured by different experimental methods. Using such data, both the VED and the difference electron densities (DED) are calculated here. Comparison with theoretical densities shows that the VED is characterized by covalent, ionic and metallic contributions. The DED constructed from GaAs and Ge data demonstrates the electronic response caused by a "protonic" charge transfer between both f.c.c. sublattices as well as the transition from a purely covalent to a mixed covalent-ionic bond. Especially the charge-density accumulation between nearest neighbours (bond charge (BC)) depends on the distance between the bonding atoms and changes under the influence of any lattice deformation. This phenomenon is described by a BC-transfer model. Its direct experimental proof is given by measuring the variation of the scattering power of weak reflections under the influence of an external electric field. This experiment demonstrates that the ionicity of the bond changes in addition to the BC variation.

Key words: Valence charge density; GaAs; Chemical bond; Bond charge transfer; Ionicity.

1. Introduction

Most of the ground-state properties of solid-state systems depend on their valence electron density (VED). In the framework of density functional theory [1] the Hellmann-Feynman theorem connects the ionic potential $V(\boldsymbol{R}, \boldsymbol{r})$ and the VED $\varrho(\boldsymbol{R}, \boldsymbol{r})$ with the total energy of system,

$$E_{\text{tot}} = E[V(\boldsymbol{R}, \boldsymbol{r}), \varrho(\boldsymbol{R}, \boldsymbol{r})]. \tag{1}$$

$\boldsymbol{R}$ stands for the ionic positions and $\boldsymbol{r}$ for the electron coordinates. After the complete solution of the variational problem for the wave functions that are used in the calculation of the density, (1) can be written in separate terms of ϱ and V,

$$E_{\text{tot}} = E_{\text{kin}}[\varrho(\boldsymbol{r})] + E_{\text{ii}}[V(\boldsymbol{R})] + E_{\text{ee}}[\varrho(\boldsymbol{r})] + E_{\text{ei}}[V(\boldsymbol{R}), \varrho(\boldsymbol{r})] + E_{\text{xc}}[\varrho_{\text{tot}}(\boldsymbol{r})]. \tag{2}$$

E_{kin} denotes the kinetic energy of electrons, E_{ii} stands for the ion-ion, E_{ee} for the electron-electron, E_{ei} for the electron-ion and E_{xc} for the exchange and correlation energy of the total electron density $\varrho_{\text{tot}}(\boldsymbol{r})$.

E_{tot} is minimum for the correct VED for given R and ϱ and corresponds to the ground-state energy. The absolute minimum of E_{tot} as a function of $\boldsymbol{R}$ defines the equilibrium position $\boldsymbol{R} = \boldsymbol{R}_0$. Any change of E_{tot} with respect to a deformation coordinate $\boldsymbol{u} = \boldsymbol{R} - \boldsymbol{R}_0$ is described by the interatomic potential, which may be expanded into a power series. In X-ray crystal structure analysis of diamond and zincblende-structure materials, the one-particle potential approximation is often used [2],

$$E(\boldsymbol{u}) = \boldsymbol{E}(\boldsymbol{R}) - E(\boldsymbol{R}_0) = \alpha u^2 - \beta u^3 + \ldots. \tag{3}$$

In this case the power coefficients α and β are related to the reciprocal of the mean-square displacements and the anharmonicities of atomic vibrations, respectively.

The experimental determination of the VED of the thermal-equilibrium state and the measurement of the VED variation for any lattice deformation is of fundamental interest for the understanding of the connections between structure and physical properties in the solid state.

The aim of this paper is to discuss the current accuracy in the experimental VED. The limits of our quantitative knowledge are reviewed and the principal directions for its improvement are indicated (part 2). The transition between the purely covalent and the mixed covalent-ionic bond is studied using the difference density between GaAs and Ge data (part 3). The

* Presented at the Sagamore X Conference on Charge, Spin, and Momentum Densities, Konstanz, Fed. Rep. of Germany, September 1–7, 1991.

Reprint requests to Dr. U. Pietsch, Universität Potsdam, FB Physik, Am Neuen Palais 10, D-O-1571 Potsdam, Fed. Rep. of Germany.

0932-0784 / 93 / 0100-0029 $ 01.30/0. – Please order a reprint rather than making your own copy

VED and difference electron density (DED) are calculated by a semiempirical density model (part 4), which describes the covalent bond by the overlap between the bonding wave functions. Using this model, the bond charge (BC) variation is explained for a deformed lattice (part 5). The experimentally observed BC-variation is discussed (part 6) and applied to solid solutions (part 7).

2. The "Static" VED for GaAs

In principle, the total electron density may be constructed by the Fourier transform of measured X-ray structure amplitudes $F(h, k, l)$. The VED and the DED can be obtained from the difference between the measured $F_{\text{exp}} \cdot e^{i\varphi_{\text{exp}}}$ and theoretical structure amplitudes calculated quantum-mechanically for the closed core states, $F_c \cdot e^{i\varphi_c}$, or for complete spherical shells of atoms, $F_o \cdot e^{i\varphi_o}$, i.e.

$$\Delta\varrho(\boldsymbol{r}) = \frac{1}{a^3} \sum_{-h_c}^{h_c} \sum_{-k_c}^{k_c} \sum_{-l_c}^{l_c} \Delta F(\boldsymbol{H}) \cdot e^{2\pi i \boldsymbol{H}\boldsymbol{r}} \tag{4}$$

with

$$\boldsymbol{H} = h\boldsymbol{a}^* + k\boldsymbol{b}^* + l\boldsymbol{c}^*,$$

$$|\boldsymbol{H}| = \frac{1}{a}\sqrt{h^2+k^2+l^2}, \quad h, k, l = \text{Miller indices}$$

and

$$\Delta F(\boldsymbol{H}) = \begin{cases} F_{\text{exp}}\, e^{i\varphi_{\text{exp}}} - F_o\, e^{i\varphi_o} & \text{for DED,} \\ F_{\text{exp}}\, e^{i\varphi_{\text{exp}}} - F_c\, e^{i\varphi_c} & \text{for VED.} \end{cases} \tag{5}$$

$F_{c,o}$ and the scattering phases $\varphi_{c,o}$ can be calculated from the data given in [3]. The lattice parameter a is known very accurately [4].

The Fourier sum in (4) is not carried through to infinity but up to a certain $H = H_c$ where the difference between F_{exp} and F_{theo} is negligibly small.

GaAs crystallizes in the noncentrosymmetrical zinc-blende structure ($F\bar{4}3m$). The Ga and As atoms occupy two different f.c.c. sublattices. There are four different classes of structure amplitudes [5]

$$F = 4(f_{\text{Ga}} + \alpha f_{\text{As}}) \tag{6}$$

with

$$\alpha = \begin{cases} 1 & \text{for } h+k+l = 4n \quad \text{(s)}, \\ -1 & \text{for } h+k+l = 4n-2 \quad \text{(w)}, \\ i & \text{for } h+k+l = 4n-1 \quad \text{(m)}, \\ -i & \text{for } h+k+l = 4n+1 \quad \text{(m)}. \end{cases} \tag{7}$$

Owing to the close neighbourhood of Ga and As in the periodic table of elements, F differs extremely between the strong (s) and moderate (m) reflections on the one hand and the week (w) reflections, on the other. However, both groups are differently sensitive in different regions in the VED. The (s)s and (m)s measure primarily the density near the atoms, whereas the (w)s are related to the interatomic region. For an accurate VED and DED, highly precise experimental data for F_{exp} with errors less than 1% are required. This cannot be achieved for both groups of reflections using the same experimental concept. Since the weak reflections fulfil the kinematic limit, standard techniques of the X-ray crystal-structure analysis can be used [6, 7]. In contrast to that, (s) and (m) reflections have to be evaluated by taking into account dynamical scattering effects in order to avoid extinction problems. This has been performed by Kobayashi et al. [8] using Pendellösung interferences with white radiation, and by Matsushita and Hayashi [9] using the angular width of reflection curves. In spite of their high individual accuracy, both data sets disagree on the absolute scale and are limited in the magnitude of the scattering vector by $\sin\theta/\lambda < 0.81\,\text{Å}^{-1}$ and $< 0.61\,\text{Å}^{-1}$, respectively.

The VED and DED have been calculated [10] using the data from [9] and [7]. Owing to the non-centrosymmetry of the structure in conjunction with dispersion, the Friedel law is broken and $|F(hkl)|$ and $|F(\bar{h}\bar{k}\bar{l})|$ are different. This is taken into account for weak reflections, but not for the others. Furthermore, the density calculation can be performed only after correction of the experimental structure amplitudes for anomalous dispersion and anharmonicity effects. Owing to the well-known phase problem of structure analysis, this is not possible without applying a density model. In the present case the "static" bond-charge model was used, which takes into account the charge accumulation between nearest neighbours by an additional scattering "particle" [7].

The so calculated VED and DED are shown in Figs. 1 and 2. In both plots the Ga atoms are located in the upper corners, and the As atoms are near the centre of the Figures. The chemical bond can be described by three contributions. The covalent part is characterized by the charge accumulation between nearest neighbours. Caused by the ionicity, its maximum is shifted from the middle of the Ga–As bond towards the As atom. The ionicity leads also to the higher charge density near As in comparison to Ga. This, in turn, is the reason for the higher shift of the density maximum in the VED compared with the DED. At least the positive DED at the Ga and As sites

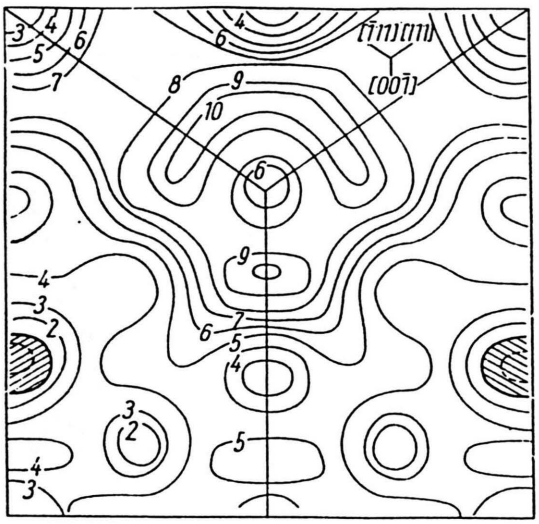

Fig. 1. VED plot in the (110)-plane of GaAs. Two Ga atoms are located in the left and right corners at the top; an As atom is near the centre. The density contours are separated by steps of about $0.084 \cdot 10^{30}$ electrons/m^3. Hatching indicates "positive" density regions.

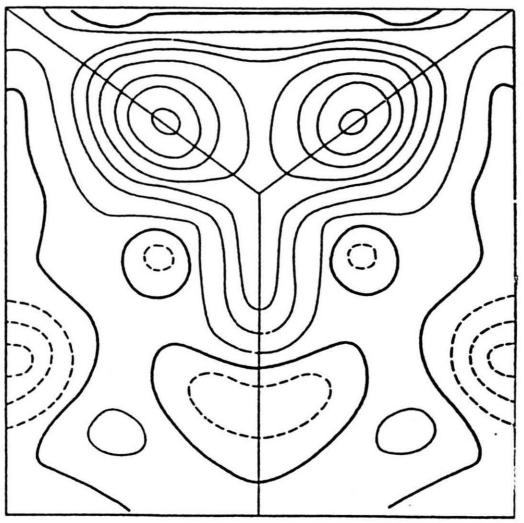

Fig. 2. DED plot for GaAs in the same geometry as in Fig. 1, contours in steps of about $0.024 \cdot 10^{30}$ electron/m^3. The zero line is thick, negative contours are dashed.

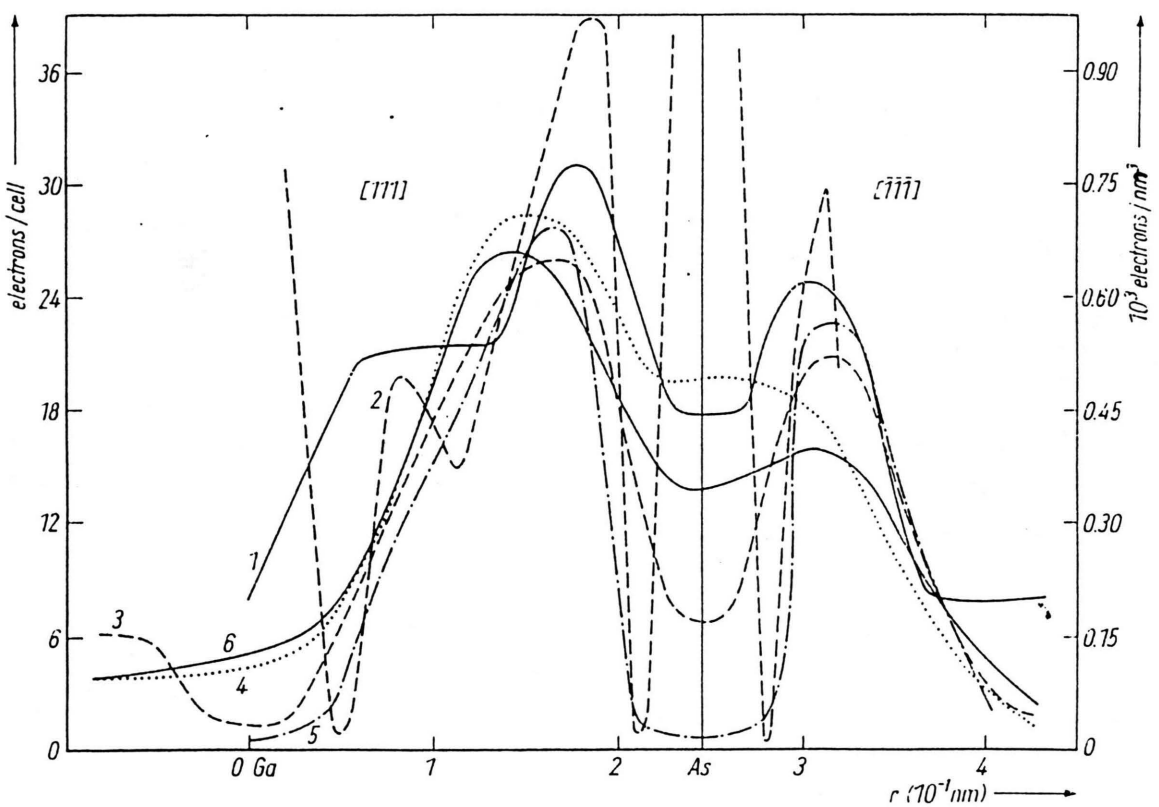

Fig. 3. The VED of GaAs along the line between nearest neighbours in comparison with other density models: (1) experiment, (2) from [6], (3) from [11], (4) from [12], (5) from [13] and (6) from [14].

indicates a moderate metallic contribution to the chemical bond.

However, there are some unexpected features in the VED that may be explained by experimental and systematic errors. The density maximum in the [001]-direction and the "negative" VED in the antibonding direction can be caused by the limited data set. A comparison of the experimental density with theoretical pseudopotential calculations (Fig. 3) leads to a qualitative agreement in the bonding region, but larger differences elsewhere. Quantitatively the densities differ by about 10–20%. This discrepancy has not been solved during the last five years. The accuracy of the experimental density can only be improved by using a more extended data set, by taking the polarity for the (m) structure amplitudes into account and by using more accurate values for anomalous dispersion, temperature factors and anharmonicity. Especially the latter is only roughly known. For weak reflections and $|\boldsymbol{H}| > 5a^{-1}$ it is approximately five times higher than the influence [15] of the bond charge. Thus, the measurement of more accurate anharmonicity constants is the key problem for the improvement of the experimental VED in GaAs.

3. The Density Difference between GaAs and Ge

Germanium as a diamond-type semiconductor has covalent bonds, and its charge-density maxima are located exactly in the middle between nearest neighbours. For GaAs the ionicity must be taken into account, additionally. The DED between GaAs and Ge data accordingly allows to study the change in the bond charge distribution caused by a "protonic" charge transfer between both f.c.c.-sublattices.

Such a study was undertaken by using the X-ray structure amplitudes for Ge measured at the same laboratory as the GaAs data [16]. This ensures the same level of accuracy. In contrast to GaAs, the "weak" reflections of Ge depend only on the BC. They were measured accurately by Roberto and Battermann [17]. The calculated GaAs–Ge DED is shown in Figure 4. Following Baur et al. [18], the electronic response is expanded in linear and quadratic terms. Whereas the linear part comes from the charge transfer between the spherical ions, the quadratic term describes the decreasing BC amount. Generally, the transition between covalent and ionic bond is characterized by a parabolic decrease of the covalent BC

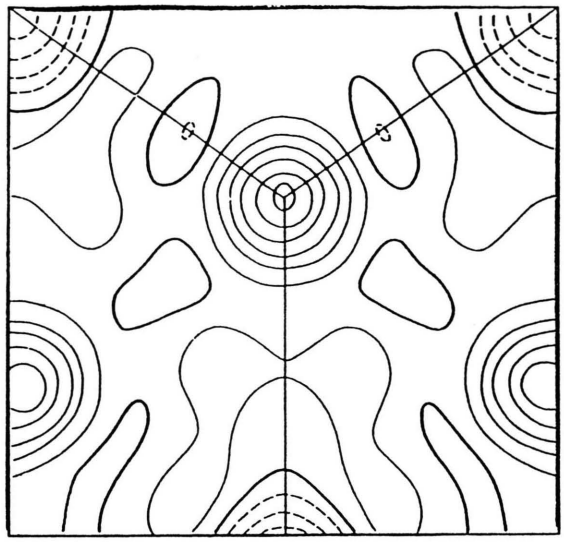

Fig. 4. Difference density between GaAs and Ge as calculated from X-ray scattering data. The geometry is the same as in Fig. 1. Contours in steps of about $0.3 \cdot 10^{30}$ electrons/m^3.

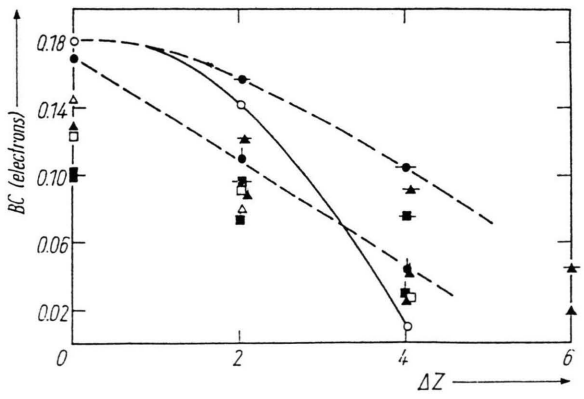

Fig. 5. The BC vs. the difference in the atomic numbers of the constituents, ΔZ, as calculated by the model of Linear Superposition of Two-Electron Molecules [21]. Circles are for the series Si–AlP–MgS [18], triangles for Ge–GaAs–ZnSe–CuBr and squares for Sn–InSb–CdTe. The full symbols have been obtained using different assumptions about the dehybridization of the valence orbitals.

with increasing difference of the nuclear charges, ΔZ, (Fig. 5) and a shift of the BC from the centre between nearest neighbours towards the anion.

4. "Realistic" Modeling of the VED

The multipole expansion has often been used for modelling the VED of covalently bound materials [19],

[20]. The redistribution of valence electrons is described by multipole functions centred at atomic sites. A different possibility is given by the "static" BC model. In this case the BC is considered like a scattering "particle" [7]. The disadvantage of both models consists in their rigidity, which does not allow to describe any deformation of the VED without redetermination of the parameters.

In contrast, the model LISTEM (Linear Superposition of Two Electron Molecules) describes the covalent bond as quantum mechanical overlap of bonding wave functions. In order to generate the complete crystal with its tetrahedral co-ordination and eight electrons in the primitive lattice cell, "molecules" possessing two electrons and two effective core charges are studied. The chosen ansatz function of the molecular density,

$$\varrho_{ij}(\boldsymbol{r}) = \frac{1}{1+S_{ij}^2} \cdot [A_i|\psi_i(\boldsymbol{r}-\boldsymbol{R}_i)|^2 + A_j|\psi_j(\boldsymbol{r}-\boldsymbol{R}_j)|^2 + 2\sqrt{A_i A_j}\, S_{ij}\psi_i(\boldsymbol{r}-\boldsymbol{R}_i)\,\psi_j(\boldsymbol{r}-\boldsymbol{R}_j)], \quad (8)$$

contains two centres i and j which are separated by the next-neighbour distance $R = |\boldsymbol{R}_j - \boldsymbol{R}_i|$. The total VED of the crystal is obtained by

$$\varrho_{\text{crystal}}(\boldsymbol{r}) = \sum_{i,j} \varrho_{ij}(\boldsymbol{r})\, D(\boldsymbol{r}, \boldsymbol{r}'). \quad (9)$$

The operator $D(\boldsymbol{r}, \boldsymbol{r}')$ forces the tetrahedral co-ordination of the "molecules" with respect to any bond. According to the V.B. approximation [22], the density is assumed to be a weighted resonance structure among the neutral A^0B^0 and the ionic structures A^+B^- and A^-B^+. The population parameters A_{ij} allow to determine the effective charge of the ions as well as the ionicity of the bonds. The total VED is characterized by spherical (ionic)

$$\varrho_{\text{ion}_{i,j}}(\boldsymbol{r}) = 4A_{i,j}|\psi_{i,j}(\boldsymbol{r}-\boldsymbol{R}_{i,j})|^2 \quad (10)$$

and nonspherical (bond charge) contributions

$$\varrho_{\text{BC}}(\boldsymbol{r}) = 2\sqrt{A_i A_j}\, S_{ij}\psi_i(\boldsymbol{r}-\boldsymbol{R}_i)\,\psi_j(\boldsymbol{r}-\boldsymbol{R}_j). \quad (11)$$

The total amount per bond is given by

$$\text{BC} = \frac{2S_{ij}^2}{1+S_{ij}^2} \quad (12)$$

and depends on R and the angle Θ_{kl} between the bonding orbitals centred on the same ion. S_{ij} is the overlap integral between the chosen hybridized model wave functions

$$\psi_{i,j}(\boldsymbol{r}-\boldsymbol{R}_{i,j}) = (1/N_{i,j})^{1/2}(\mu|s\rangle + |sp^x\rangle), \quad x=\lambda^2, \quad (13)$$

centred on the atomic sites $\boldsymbol{r}=\boldsymbol{R}_i$ and $\boldsymbol{r}=\boldsymbol{R}_j$.

The $N_{i,j}$ are normalization constants. The hybridization parameter λ is determined from the orthogonality condition

$$1 + \lambda_k \lambda_l \cos\vartheta_{kl} = 0. \quad (14)$$

In order to describe the metallic character of the bond, which increases from C to α-Sn, the $|s\rangle$-like character of $\psi_{i,j}$ is enhanced as quantified by the parameter μ. For the group-IV elements the screening constants of the $|s\rangle$- and $|p\rangle$-like basis functions are fitted to the experimental VED. The use of Gaussians is solely justified by their simple mathematical properties.

At the transition from diamond to zincblende-structure compounds both the "effective charge" of ions and the dehybridization of bonding orbitals have to be considered. It is known qualitatively that the sphericity of ions increases in the order Ge–GaAs–ZnSe–CuBr up to the phase transition between zincblende and rock-salt structures [23]. Since exact values are unknown, a linear dehybridization, i.e. an increase of μ_i, was assumed. The screening constants of the ions were fitted self-consistently to the transferred charge Δz between neighbouring orbitals. Considering four next neighbours, the effective charge e^* of the compound is

$$e^* = -4\Delta z. \quad (15)$$

The ionicity I of the compound can be quantified in terms of the BC displacement off the centre between nearest neighbours,

$$I = \frac{A(R_{\text{BC}} - R/2)}{R/2}. \quad (16)$$

After a least-squares fit of 24 zincblende-structure compounds, the constant in (16) is found to be $A = 2.40 \pm 0.10$ [21].

The VED calculated by using LISTEM is shown in Figure 6. It exhibits all significant features of the semicovalent bond. There are the displaced BC maximum, the transferred ionic charge and the metallicity of the bond. Owing to the simple Gaussians used, the BC shape is somewhat sharper and the BC maximum is higher than in the experiment (Figure 1). The BC density (Fig. 7) is calculated by using only the nonspheri-

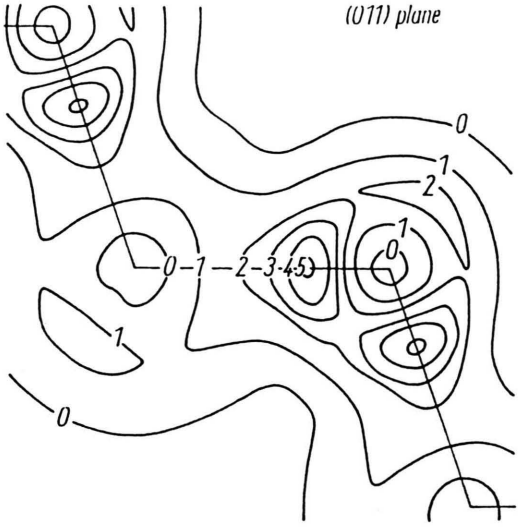

Fig. 6. The VED of GaAs calculated by LISTEM. The maximum density amounts to $1.12 \cdot 10^{30}$ electrons/m^3. The contour distance is $0.22 \cdot 10^{30}$ electrons/m^3.

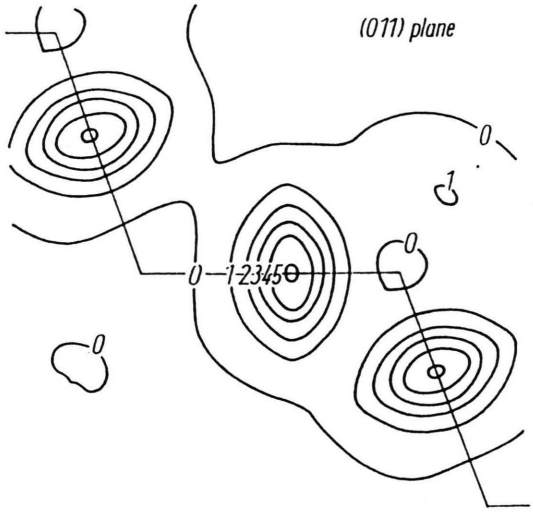

Fig. 7. The BC density (DED) of GaAs calculated by LISTEM. The maximum of density amounts to about $0.12 \cdot 10^{30}$ electrons/m^3. The contour distance is $0.022 \cdot 10^{30}$ electrons/m^3.

cal parts (11) of the density. It corresponds to the DED shown in Figure 2.

Note that the sum of BC and Δz corresponds to the "bond charge" $2e/\varepsilon_0$ of Van Vechten and Phillips [24] that results from a linear-screening concept of a bare pseudopotential in a simple two-band scheme of semiconductors.

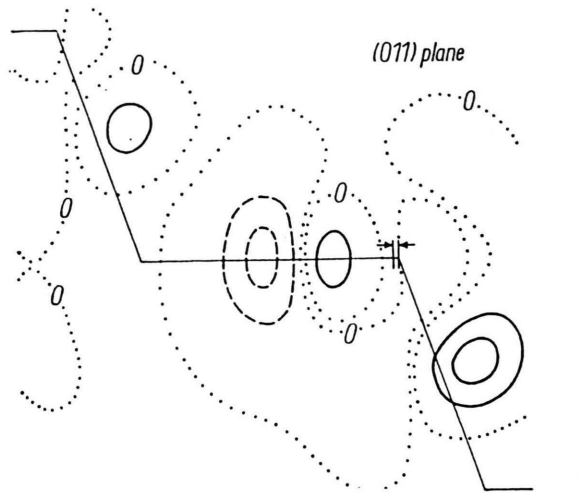

Fig. 8. The BC polarization density of GaAs caused by an As atom displaced by about 0.053 nm with respect to the rigid lattice. The zero line is dotted, the regions of decreased electron density are dashed.

5. VED of Deformed Lattices (BC Transfer)

LISTEM is able to describe the change of the BC caused by any deformation of the lattice. Without any variation of screening constants, the BC is expanded as

$$\begin{aligned} \mathrm{BC} &= \mathrm{BC}_0 + \gamma_1 \Delta R + \gamma_2 (\Delta R)^2 + \delta_1 \Delta\vartheta + \delta_2 (\Delta\vartheta)^2 + \ldots \\ &= \mathrm{BC}_0 + \bar{\gamma}_1 \Delta R + \bar{\gamma}_2 (\Delta R)^2 \end{aligned} \tag{17}$$

in terms of the changes in next-neighbour distances $\Delta R = R - R_0$ and bond angles $\Delta\vartheta$.

An increased ΔR leads to a decreased overlap. A change of $\Delta\vartheta$, on the other hand, varies the $|sp^3\rangle$ character of bonding orbitals and thus the overlap charge, too.

It is often sufficient to use the effective parameters γ_1 and γ_2 (Table 1). The DED between the deformed BC density and the undeformed one is shown in Figure 8. Owing to a displacement of the As atom ($\Delta R =$ 0.053 nm), the central bond length is stretched, and those of the bonds lying nearly perpendicular to it are compressed. This results in a decreased overlap at the central bond but an increased BC at the others. "Bond charge" is transferred from the stretched to the compressed bond. Baldereschi and Maschke [25] have first discovered theoretically that the BC transfer is necessary to explain the TA (x) phonon softening in silicon. The values of the corresponding parameters fitted by LISTEM are of the same order of magnitude as those

Table 1. BC transfer constants for a thermal displacement with respect to the rigid lattice, calculated by LISTEM. (γ_1 in units of 10^{10} electrons/m^3, γ_2 in 10^{10} electrons/m^2.)

Compound	Anion displacement		Cation displacement	
	$\bar{\gamma}_1$	$\bar{\gamma}_2$	$\bar{\gamma}_1$	$\bar{\gamma}_2$
Si	−0.19	−0.09	−0.19	−0.09
Ge	−0.19	+0.07	−0.19	+0.07
GaP	−0.18	−0.04	−0.16	−0.05
GaAs	−0.18	−0.07	−0.16	−0.06
GaSb	−0.17	+0.13	−0.15	+0.05
ZnS	−0.07	−0.08	−0.06	+0.07
ZnSe	−0.10	+0.10	−0.09	+0.08
ZnTe	−0.13	+0.13	−0.11	+0.10

Table 2. The relative variation of the scattering intensity of "weak" reflections of GaAs under the influence of an external electric field of about 40 kVcm^{-1} parallel to the [111]-direction in units of 10^{-4}. Theoretical values were calculated using Eq. (18).

Reflection	$(\Delta I/I)_{\text{exp}}$	$(\Delta I/I)_{\text{theo}}$
(222)	6.8 (1.0)	7.0
(222)	2.1 (1.0)	4.3
(442)	7.4 (0.8)	4.4
(442)	6.6 (0.8)	3.2
(622)	−0.8 (0.9)	−0.6
(622)	−0.9 (0.9)	−1.1

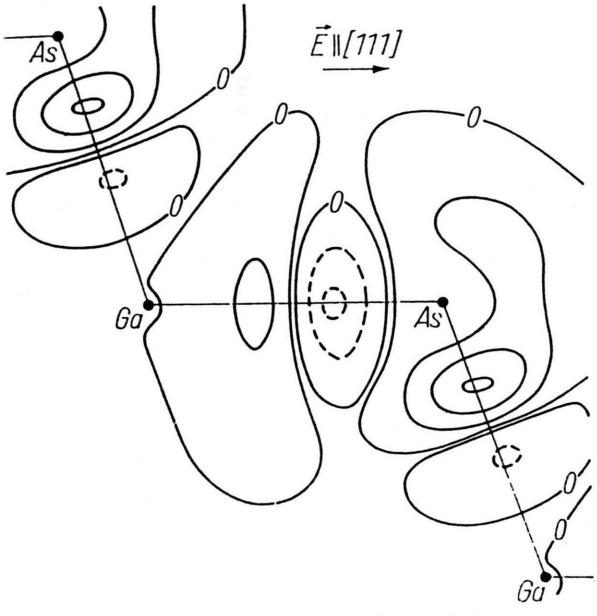

Fig. 9. The BC polarization density of GaAs induced by an applied external electric field of about 40 kVcm^{-1}. Contours are drawn at $6 \cdot 10^{24}$ electrons/m^3 step-width.

given by self-consistent pseudopotential calculations. It enables a semiempirical calculation of any deformation density of zincblende-structure compounds.

6. The Experimental Proof of BC Transfer

The validity of the BC transfer concept may be verified experimentally by measuring BC-dependent X-ray structure amplitudes under the influence of externally induced perturbations of the lattice. For silicon the "forbidden" (222)-reflection has been measured under hydrostatic pressure P [26]. It depends solely on the BC and increases as a function of P up to $P \approx 100$ kbar. This can be completely explained by the increasing overlap of bonding orbitals [27]. Unfortunately, the experiment is not definite because of the large fluctuation of the experimental values.

More judicious was an experiment proposed by Fujimoto [28]. Because of the high resistivity introduced by chromium doping, a high external electric field can be applied to GaAs. Using $E = 40$ kV cm^{-1}, the variation of weak reflections was measured using a modulation technique [29]. The relative variation of the scattering intensity is shown in Table 2. In the kinematic limit it can be interpreted as the derivative of the structure amplitude ΔF,

$$\begin{aligned}\Delta F(\boldsymbol{H}) = &\sum_{j=1}^{8} f_i \, e^{-2\pi i \boldsymbol{H} \boldsymbol{r}_j} \cdot 2\pi \boldsymbol{H} \Delta \boldsymbol{r}_j \\ &+ \sum_{j=1}^{8} f_j \, e^{-2\pi i \boldsymbol{H} \boldsymbol{r}_j} \cdot \Delta f_j \\ &- \sum_{j=1}^{16} f_{\text{BC}} \, e^{-2\pi i \boldsymbol{H} \boldsymbol{x}_j} \cdot 2\pi \boldsymbol{H} \Delta \boldsymbol{x}_j \\ &+ \sum_{j=1}^{16} f_{\text{BC}} \, e^{-2\pi i \boldsymbol{H} \boldsymbol{x}_j} \cdot \Delta f_{\text{BC}}, \end{aligned} \tag{18}$$

with respect to the change of ion positions, $\Delta \boldsymbol{r}_j$, change of atomic form factors, Δf_j, the BC shift $\Delta \boldsymbol{x}_i$, and the changed overlap. The ionic displacement calculated from the piezoelectric constant gives rise to ΔF two orders of magnitude smaller than measured and may be neglected together with the second term. Only the third and fourth terms are considered. The calculated polarization density is shown in Figure 9. Applying the positive pole on the left-hand side, the central BC is shifted towards the centre between next neighbours. Its ionicity decreases, and its BC amount is enhanced. On the other hand, as the ionicity of the noncentral bonds increases, their BC decreases ac-

cording to the parabolic dependence on ΔZ (Figure 5). The induced shift of BC against the field amounts to $(1.2 \pm 0.3) \cdot 10^{-5}$ nm, which corresponds to a change in ionicity of about 0.02%.

A repetition of the experiment for silicon (222) yields

$$\frac{\Delta I}{I} = \left|\frac{\Delta F}{f}\right|^2 = +(0.98 \pm 0.40) \cdot 10^{-4} \approx 0. \quad (19)$$

In contrast to GaAs, the BC of all the bonds is shifted away from the bond centre. Following Fig. 5, the variation of the amount of BC near $\Delta Z = 0$ is very small and cannot be measured for the applied field strength of $E = 5\ \mathrm{kV\,cm^{-1}}$ [30].

However, the electric-field-induced variation of the X-ray structure amplitude demonstrates the validity of the BC transfer model for the interpretation of the density variation in semi-covalently bound materials.

7. VED Variation in Solid Solutions

For a solid solution $A_{1-x}B_xC$, two different kinds of VED redistribution have to be considered [31]. First, the electronegativities of the A and B atoms localized at the same sublattice are different and cause a charge transfer within this sublattice. This results in a different electron population at the A–C and B–C bond, respectively. Secondly, the amount of the bond charge is varied in comparison to the isolated A–C and B–C compounds caused by the different actual nearest-neighbour distances.

According to EXAFS experiments [32], the nonsubstituted f.c.c. sublattice is deformed in such a way that the elastic energy caused by stretching/compressing the A–C bond and, vice versa, compressing/stretching the B–C bond is minimized. The displacement of the C atom with respect to its ideal position can be explained by simple elastic models [33].

The respective charge redistribution may be calculated using the BC transfer constants (Table 1). It turns out that the sum of the BCs in solid solution is only slightly different as compared with the sum of isolated BCs [34]. Moreover, the intrinsic deformation is distributed statistically among the four possible directions.

Therefore, an ordinary X-ray scattering experiment cannot distinguish between the real deformed and assumed virtual crystal. However, the intrinsic deformation of the tetrahedra changes the elastic properties of the solid solution. This explains the nonlinearity of the thermal expansion coefficient for $GaAs_{1-x}P_x$, e.g. [35].

8. Summary

Using recently available X-ray structure amplitudes the calculated VED verifies qualitatively the theoretical model of the ionic-covalent bond in GaAs. Owing to the limited number of experimental data and the low accuracy of the correction parameters, the quantitative knowledge of the VED is not better than 20%. However, a realistic semiempirical simulation has to include metallic, ionic and covalent contributions. The model LISTEM is here proposed. It explains the covalent bond as a consequence of the overlap charge between bonding orbitals. It allows, moreover, a simulation of the VED of tetrahedrally bonded zinc-blende-structure compounds and provides estimates for ionicity, BC, etc. A further advantage is given by the description of the VED changes induced by any deformation of the lattice. The BC transfer is proposed as the important part of the VED variation. It can be observed experimentally by measuring the electric-field-induced variation of structure amplitudes.

Starting with the knowledge about the VED of pure binary compounds, the BC transfer must be taken into account in solid solutions with regard to their composition as well as when transferring the corresponding bond into any other compound.

The authors thanks the Alexander v. Humboldt Foundation for its support and K. Unger (Leipzig), J. Mahlberg (Zwickau), R. P. Ozerov and V. G. Tsirelson (Moscow) for their helpful collaboration.

[1] P. Hohenberg and W. Kohn, Phys. Rev. **136,** 864 (1964). – W. Kohn and L. J. Sham, Phys. Rev. **140,** A 1133 (1965). – R. G. Parr and W. Yang, Density-Functional Theory of Atoms and Molecules, Oxford University Press – Clarendon Press, New York and Oxford 1989.
[2] B. Dawson and B. T. M. Willis Proc. Roy Soc. London A **298,** 307 (1967).
[3] International Tables of X-ray Crystallography, Vol. 4, Kynoch Press, Birmingham 1974.
[4] O. Madelung (ed.), Landolt/Börnstein, Vol. 17 a, Springer-Verlag, Berlin 1982.
[5] B. Dawson, Proc. Roy Soc. London A **298,** 379 (1967).
[6] D. H. Bilderback, Thesis, Purdue University, West Lafayette 1975.
[7] U. Pietsch, phys. stat. sol. (b) **103,** 93 (1981).
[8] K. Kobayashi, T. Takama, and S. Sato, Jap. J. Appl. Phys. **27,** 1377 (1988).
[9] T. Matsushita and J. Hayashi, phys. stat. sol. (a) **41,** 139 (1977).
[10] U. Pietsch, V. G. Tsirelson, and P. R. Ozerov, phys. stat. sol. (b) **138,** 47 (1986).
[11] J. Ihm and J. D. Joanuopoulos, Phys. Rev. B **24,** 4191 (1981).
[12] A. Baldereschi, K. Maschke, A. Milchev, R. Pickenhain, and K. Unger, phys. stat. sol. (b), **108,** 511 (1981).
[13] C. S. Wang and B. M. Klein, Phys. Rev. B **24,** 3393 (1981).
[14] J. C. Chelikowsky and M. L. Cohen, Phys. Rev. B **14,** 556 (1976).
[15] U. Pietsch, phys. stat. sol. (b) **111,** K7 (1982).
[16] T. Matsushita and K. Kohra, phys. stat. sol. (a) **24,** 531 (1974).
[17] J. B. Roberto, B. W. Ballermann, and D. Keating, Phys. Rev. B **9,** 2590 (1974).
[18] J. Baur, K. Maschke, and A. Baldereschi, Phys. Rev. B **27,** 3720 (1983).
[19] P. F. Price, E. N. Maslen, and S. L. Mair, Acta Cryst. A **34,** 183 (1978).
[20] M. Spackmann, Acta Cryst. A **42,** 271 (1986).
[21] U. Pietsch, phys. stat. sol. (b) **120,** 183 (1983), **126,** 595 (1984), **128,** 439 (1985).
[22] L. Pauling, The Nature of the Chemical Bond, Cornell University Press, Ithaca 1960.
[23] E. Antončik and B. L. Gu, Physica Scripta **25,** 835 (1982).
[24] J. A. Van Vechten and J. C. Phillips, Phys. Rev. B **2,** 2160 (1970).
[25] A. Baldereschi and K. Maschke, Proc. Int. Conf. on Physics of Semicond., Edinburgh 1976.
[26] D. R. Yoder-Short, R. Collela, and B. A. Weinstein, Phys. Rev. Lett. **49,** 1438 (1982).
[27] U. Pietsch, phys. stat. sol. (b) **120,** 183 (1983).
[28] I. Fujimoto, Jap. J. Appl. Phys. **19,** L347 (1980).
[29] U. Pietsch, J. Mahlberg, and K. Unger, phys. stat. sol. (b) **131,** 67 (1985).
[30] U. Pietsch and K. Unger, phys. stat. sol. (b) **143,** K95 (1987).
[31] U. Pietsch, phys. stat. sol. (b) **134,** 21 (1986).
[32] J. C. Mikkelson and J. B. Boyce, Phys. Rev. Lett. **49,** 1412 (1982).
[33] T. Fukui, J. Appl. Phys. **57,** 5188 (1985).
[34] U. Pietsch, phys. stat. sol. (b) **107,** 185 (1981).
[35] U. Pietsch, phys. stat. sol. (b) **133,** 483 (1986).